

Systematic switching study of transformer inrush current: simulations and measurements

N. Chiesa, H. K. Høidalen

Abstract—The verification of a transformer model for the representation of transient behaviors such inrush and ringdown is not trivial as several parameters may influence measurements and simulations. The purpose of this paper is to suggest a laboratory testing strategy and to present an enhanced transformer model. A special emphasis is given to parameters estimation. The objective is to be able to obtain most of the model data directly from standard test report data. Design data are used to verify the parameters and to have a better estimation of scaling factors. The model is verified against few measurements and good agreement is observed for residual flux, inrush current first peak and decay.

Keywords: Power transformer, inrush current, ringdown transient, residual flux, EMTP/ATP modeling.

I. INTRODUCTION

THE power transformer is an essential component in power systems. The standard models used to predict its transient behavior are however rather poor due to both lack of data, measurements, and knowledge. Transient situations of special concern spans from lightning impulse stresses and winding resonance to inrush currents and ferroresonance. Thus, the transformer modeling for transient analysis is a great challenge.

Transformer modeling is an active topic in the research community with papers published on different issues. References [1]–[3] present a comprehensive and up to date review of transformer models for electromagnetic transients. Based on the importance of the iron core representation, transformer models for network simulation can be divided in four main categories:

- 1) Steady state models; core representation is not critical and can usually be neglected in load flow, short circuit and any steady-state calculations.
- 2) Models based on matrix and circuit representation; the iron core behavior can be linearized, however simulation errors occur when the core is driven in the saturation area. This approach is used in BCTRAN component in ATP-EMTP, [4]. To improve the core representation, excitation can be extracted from the main circuit and an additional nonlinear circuit can be externally attached at the model terminal. In the classical Saturable Transformer model the magnetizing branch is added at the internal star-point, [4].

- 3) Topologically correct models are based on the transformer geometry and duality theorem; one of the first model offered in a simulation package to take advantage of this approach is the unified magnetic equivalent circuit (UMEC) model in PSCAD/EMTDC [5]–[7]. Another model that uses the geometry and duality approach is the hybrid transformer model [8]–[10] recently implemented in ATPDraw under the name XFMR, [11]. In these transformer models each individual limb of the magnetic circuit is represented and contributes to the magnetization characteristic. This approach can very accurately represent any type of core but requires a slightly larger set of data.
- 4) Models based on finite element methods (FEM). Such type of modeling technique can be very accurate but has the disadvantages to be valid only for a specific unit and requires huge computing resources, still retain several approximations, [12].

The scope of this paper is aimed at power transformers where inrush current phenomena is an issue related to relay setting, inrush mitigation by synchronized switching, voltage harmonic distortion, and internal mechanical stress reduction. The investigated models (UMEC and XFMR) however present limitations related to accuracy at extreme saturation and proper representation of hysteretic behavior of the core, [11]. The model proposed here is based on a topologically correct and hysteretic core, with special consideration for the behavior in extreme saturation. Model parameters are obtained from relatively standard test that are usually performed at the transformer factory before the delivery of the transformer. Few design data may become useful to accurately tune few parameters to achieve higher accuracy level, but are usually not of critical importance.

Beside the investigation of an EMTP model, the purpose of the paper is also to discuss a method for properly verifying such model with regards to inrush current measurements performed in laboratory on a distribution transformer. First the laboratory setup and the data of the transformer used as test object are presented. The EMTP model is then outlined and an overview of the parameters estimation is given. Finally, few disconnection and energization transient measurements are compared with simulations and discussed.

II. LABORATORY SETUP

A. Equipment

A distribution transformer is used for laboratory investigation. The test object is oil filled with a three-legged core. The presence of oil as insulation medium and consequently of the

N. Chiesa and H. K. Høidalen are with the Department of Electric Power Engineering, Norwegian University of Technology (NTNU), Trondheim, Norway (e-mail of corresponding author: nicola.chiesa@elkraft.ntnu.no).

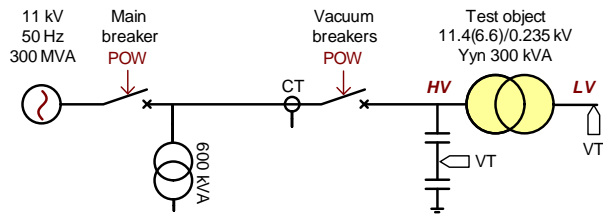


Fig. 1. Laboratory layout.

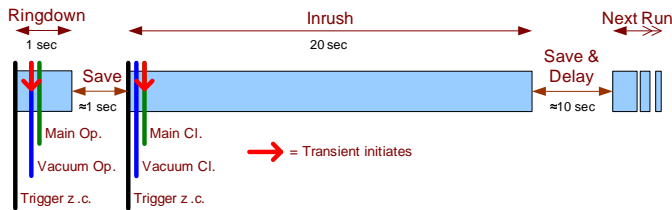


Fig. 2. Synchronized double triggering and double recording procedure.

transformer tank is important to maintain insulation distances and therefore capacitances more comparable to those in power transformers. The importance of capacitances will be described in section III-B

The transformer is rated 300 kVA 11.430/0.235 kV Yyn. The transformer is connected to a stiff 11 kV medium voltage grid (with short circuit capacity of 300 MVA) and is being energized by two sets of controlled circuit breakers as shown in Fig. 1. Both energization and de-energization transients are being recorded.

The purpose of the testing is to perform systematic measurement where the breakers operation is accurately controlled with a resolution of 1 ms. This is allowed by a stable operation time of the breakers. The main breaker installed in the laboratory is an old ABB-Sace vacuum breaker and has been tested to give stable operation time concerning the energization operation.

The evolution of the ringdown transient is complicated by stray capacitances of the cables between the main breakers and the test object, and above all by the presence of a second 600 kVA transformer energized in parallel with the test object, see Fig. 1. This transformer is not relevant to the scope of the test, but could not be easily disconnected. It has been verified that this transformer does not influence the energization transient due to the stiffness of the 11 kV network, on the other side the ringdown and the residual flux establishment of the test object is greatly influenced as the two transformer will result connected in parallel and swings together during ringdowns if only the main breaker is used. In order to decouple the ringdown of the two transformers and record only the test object response, an additional vacuum breaker is placed before the test object terminals. The main breaker and the vacuum breaker are used independently and exclusively to energize and disconnect the transformer, respectively.

Each pole of the vacuum breaker is operated independently by an electromagnetic relay and its operation time has been verified to be stable such that each pole of the breaker can be tuned to operate at a specific time with accuracy and

repeatability of 1 ms circa. The vacuum breaker is delivered by Ross Engineering Corp. (Type HB51).

A National Instrument PXI transient recorder (acquisition modules: PXI-6133 ad PXI-6122) has been used to record voltage and current on the high voltage terminals as well as induced voltage on the low voltage terminals. Signals are recorded at the sampling frequency of 100 kS/s. Digital output channels has been used to operate and synchronize the breakers with a common triggering reference.

The current on the high voltage side has been measured with high precision current transducer (LEM IT-400) based on closed loop (compensated) current transducer using fluxgate technology with claimed accuracy of 0.0033%. Such high accuracy together with a large bandwidth allowed to correctly measure steady state no-load current (less then one ampere) as well as severe inrush current with peak of several hundred amperes. The voltage on the high voltage terminal has been measured with capacitive voltage dividers with a high voltage capacitor of 200 nF. The bandwidth of such dividers has been measured to be above 1 MHz.

B. Procedure

Fig. 2 details the breaker operations and recording procedure used during the acquisition of de-energization and energization transients. The aim is to control and synchronize the breakers operations with the trigger signal. A signal synchronous to the zero crossing of the voltage-to-ground of the phase R on the high voltage side is used as trigger signal. An automated and synchronized double triggering and double acquisition procedure become necessary as the frequency of power systems is not fixed at 50 Hz but has a slow dynamic. This approach allows to perform systematic measurements with point-on-wave (POW) synchronization of the breakers. With a scanning trough a whole period (0 – 20 ms at 50 Hz) the relation of residual flux and inrush current to the switching instant can be characterized.

Each pair of de-energization/energization measurements are linked together as the ringdown transient determines the initial state of the residual flux in the transformer, being a fundamental initial condition for the following energization. The residual flux is calculated at the end of the ringdown transient by integration of the induced voltage and is assumed constant during the time delay before the energization process.

A measurement procedure evolves in six stages as follows:

- *Steady State*: The transformer is energized and in steady state (no-load).
- *Ringdown*: The ringdown sequence starts. The vacuum breaker opens and the de-energization transient initiates after the defined delay from a triggering impulse that set the POW. The main breaker also opens shortly after to be ready for the energization sequence, but has no effect on the measurements. The transient is recorded for the duration of 1 s.
- *Storing Data*: Recorded data are stored and a delay of 1 s is introduced between Ringdown and Inrush stages.
- *Inrush*: The inrush sequence starts. At the new trigger signal the vacuum breaker closes (but the transformer

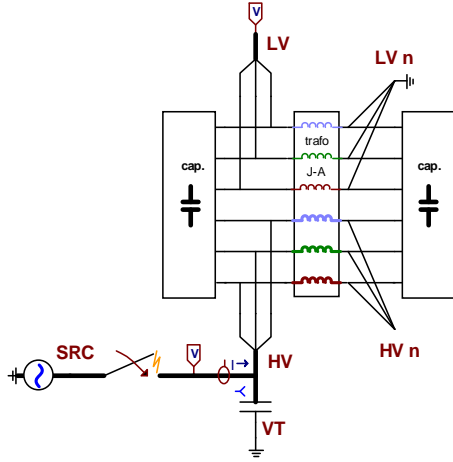


Fig. 3. Complete ATP model.

is still deenergized). The main breaker closes and the energization transient initiates after the defined delay from the triggering signal that set the POW. The transient is recorded for the duration of 20 s.

- *Storing Data & Delay:* Recorded data are stored followed by a delay of 10 s where the transformer can reach steady state.
- *Ready for Next Run:* The system is ready and in steady state. A new measurement can start.

III. EMTP MODEL

The model is developed in a similar way as the hybrid model presented in [8], [9], starting from the transformer topology and then obtain the electrical network by duality transformation. The hybrid model assumes that the leakage inductances are much smaller than the core inductance; this allows to concentrate core and leakage networks in two distinct and separate blocks. This assumption is correct under normal conditions, however become doubtful at high saturation where the differential core inductance approaches the air-core inductance with permeability μ_0 . The model proposed here has as main objective to represent inrush transient, thus such assumption has not been considered valid, leading to a fairly different final model. A compact representation of the complete model is shown in Fig. 3; each nonstandard component is detailed in the following sections.

The approach used in the hybrid model for the parameters estimation, [8], [11], is valuable and is followed here; specific parameters that may influence ringdown and inrush transients are further investigated and their estimation from test report with the help of design data is briefly discussed in the following sections.

A. Winding Resistances, Leakage Inductances, Hysteresis Core and Zero Sequence Inductances

This is the central part of the transformer model and includes winding resistances, leakage inductances, iron core model and zero sequence inductances as shown in Fig. 4.

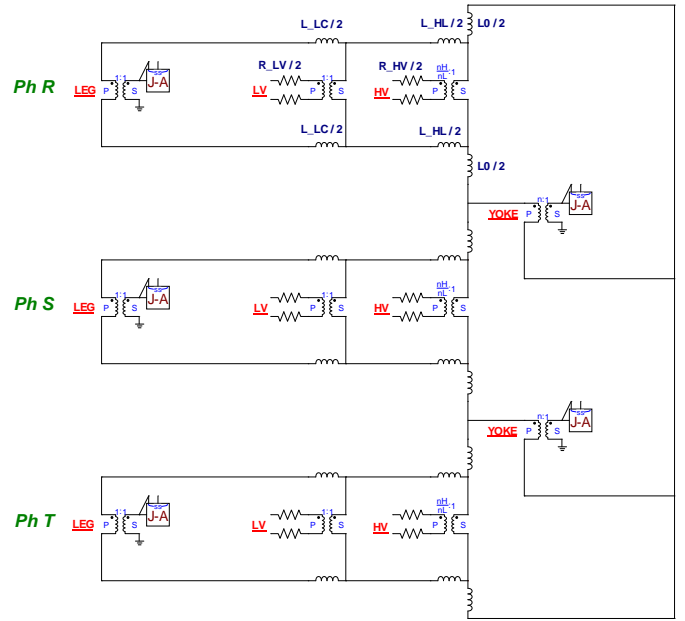


Fig. 4. Transformer model: leakage and core.

1) *Winding Resistances:* The winding resistances are concentrated at the terminals of each winding. At this stage of the development of the model, resistances have been assumed constant and frequency independent, although a Foster circuit may be used to represent frequency dependent phenomena, [8], [11]. It is common to estimate the winding resistance only based on a short-circuit measurement and then equally split the value on a per unit base between high and low voltage resistance. Here the values are estimated based in short-circuit losses and DC winding resistance measurements, expressed in per unit this is:

$$R_{AC HV} = R_{AC sc} \cdot \frac{R_{DC HV}}{R_{DC HV} + R_{DC LV}} \quad (1)$$

$$R_{AC LV} = R_{AC sc} \cdot \frac{R_{DC LV}}{R_{DC HV} + R_{DC LV}} \quad (2)$$

The splitting of the AC resistance based on DC resistance measurements usually results in per unit in $R_{AC HV} < R_{AC LV}$, thus when the transformer is energized on the high voltage side (normal situation for power and distribution transformer) the voltage drop caused by the winding resistance is smaller than when equally split, creating a higher inrush current peak.

2) *Leakage Inductances:* Leakage inductance between high and low voltage winding (L_{HL}) is calculated from the short-circuit test measurement. The approach of the $N+1$ th winding presented in [8] is used here as it provides an optimal connection point for the core. The leakage inductance between low voltage winding and core (L_{LC}) cannot however be directly measured. It is assumed as:

$$X_{LC} \approx K \cdot X_{HL} \quad (3)$$

with $K = 0.5$ being a fairly good approximation of this factor. Short-circuit reactance can be calculated from design dimension with standard equations as reported in [13] chapter 3.1. With the assumption of an infinitely thin winding on

the core surface, the reactance between low voltage winding and core can be estimated from geometry. For the specific transformer it results:

$$ATD_{HL} = 1/3 \cdot T_L \cdot D_L + T_{gHL} \cdot T_{gHL} + 1/3 \cdot T_H \cdot D_H \quad (4)$$

$$ATD_{LC} = 1/3 \cdot T_L \cdot D_L + T_{gLC} \cdot T_{gLC} \quad (5)$$

$$K = ATD_{LC} / ATD_{HL} = 0.35 \quad (6)$$

with ATD being the area of the Ampere-Turn Diagram, D_x the main diameters, and T_x the radial depths, [13]. The parameter obtained with this method is used in the model. A smaller value K results in a lower voltage drop on the low-core reactance, thus in a higher inrush current peak.

3) *Hysteretic Core*: Each section of the core is modeled separately to correctly represent the core topology of the transformer. Each of the three main legs and the two outer yokes is modeled with a Jiles-Atherton hysteretic model. The use of a true hysteretic model is of great importance to be able to predict residual fluxes in the core and automatically initialize the model by a disconnection transient. Commonly used parallel R-L iron-core representation fails to reach any residual flux value as no energy can be stored in the core, [14], [15]. The Jiles-Atherton model has been implemented in ATP as a Norton Type-94 component and the parameters are obtained by a fitting procedure from open-circuit test results and relative core dimensions as detailed in [16] where the same transformer analyzed here has been used as case study.

4) *Zero Sequence Inductances*: During unbalanced operations the flux in the three legs may not sum up to zero generating a zero sequence flux. This flux flows through the zero sequence path of the transformer, for instance from one leg and into the oil and then in the tank to reclose itself again into the core passing through the oil. Three zero sequence path can therefore be identified around each leg of a three legged transformer. Although the zero sequence path includes the tank (usually made of magnetic material), due to the dominant effect of the oil gap between the core and the tank, it can be safely assumed that zero sequence inductances are linear. Their value is best found from zero sequence test where the three phases of the transformer are energized in parallel and the total current is measured:

$$L_0 = \frac{L_{zero}}{3} \quad (7)$$

$$L_{zero} = \frac{\sqrt{2} \cdot V_{zero}}{\omega \cdot I_{zero}} \quad (8)$$

B. Capacitances

The capacitance network represented in Fig. 5 is added to each end of the coils and represents the capacitance between coils and to ground of the transformer. An accurate estimation of the transformer capacitances is important both to extend the validity of the model to higher frequency, and for a correct prediction of residual fluxes. The influence of shunt capacitance on the residual flux has been discussed in [14].

Capacitances are estimated from direct capacitance measurements from the transformer terminals. Several measurements are required as such measurements are highly susceptible to error and inaccuracy, and is always suggested to use

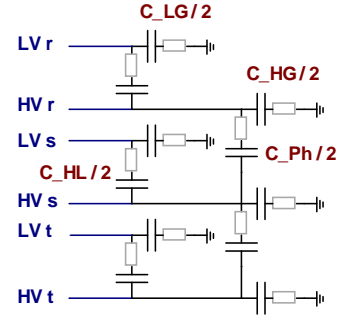


Fig. 5. Transformer model: capacitances.

redundant measurements to verify the estimated parameters. The suggested minimum set of measurement is:

- Cap. HV+LV to G

$$C_{meas} = C_{LG} // C_{HG} \quad (9)$$

- Cap. LV to G+HV

$$C_{meas} = C_{LG} // C_{HL} \quad (10)$$

- Cap. HV to G+LV

$$C_{meas} = C_{HG} // C_{HL} \quad (11)$$

- Cap. HVphR to G+LV+HVphS+HVphT

$$C_{meas} = C_{HGphR} // C_{HL} // C_{Ph} \quad (12)$$

- Cap. HVphS to G+LV+HVphR+HVphT

$$C_{meas} = C_{HGphS} // C_{HL} // C_{Ph} // C_{Ph} \quad (13)$$

- Cap. HVphT to G+LV+HVphR+HVphS

$$C_{meas} = C_{HGphT} // C_{HL} // C_{Ph} \quad (14)$$

with $//$ representing a parallel connection, and where for instance “Cap. H+L to G” means measurement of the capacitance between all the terminals of the high and low voltage windings connected together (H+L) to the transformer tank (G).

Measurements (9) to (14) together with $C_{HG} = C_{HGphR} + C_{HGphS} + C_{HGphT}$ are sufficient to estimate the capacitance values, while other coupling combinations can be measured in addition and used to verify the calculations. The capacitance C_{HL} , C_{HG} and C_{LG} estimated from solving these equations are total capacitances, while per phase capacitance values have to be used in the model. Per phase capacitances have a value of 1/3 of the total capacitances.

The measurements (12) to (14) are used to estimate the asymmetry of the capacitance to ground of the high voltage winding, however can be performed only if the three high voltage coils are accessible independently, for instance before the coupling of the neutral point in a wye connection. This is seldom possible on an already build transformer. In wye connected transformer the tap changer acts on the lower part a coil, that is where the neutral point is. The neutral point could result disconnected if the tap changer is adjusted in a intermediate location between two regular positions; such

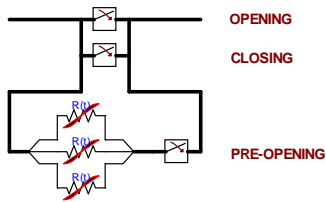


Fig. 6. Simple switch representation.

procedure has been used in the tested transformer to perform the measurements. In case of lack of such measurements C_{HG} can be equally distributed among the three phases.

Series winding capacitances has been disregarded in the model as cannot be measured from the terminal and their estimation have to be based exclusively on highly detailed winding design information, [12], [13].

An external shunt capacitance of 200 nF has been added to the high voltage terminal and represents the capacitive voltage divider.

C. Circuit Breaker

Fig. 6 details the model of the breaker used to control de-energization and energization transients in the simulation. Two ideal breakers are used for the opening and closing operation, while a third breaker in series with a non-linear time-dependent resistance is used to model the breaker transient. While the purpose of the work is not to provide a proper circuit breaker model, a simple model of the arcing phenomena showed improved results against measurements and has been adopted: a pre-opening time-dependent resistor varies exponentially between $0\ \Omega$ and $1\ \text{M}\Omega$ in $1.5\ \text{ms}$.

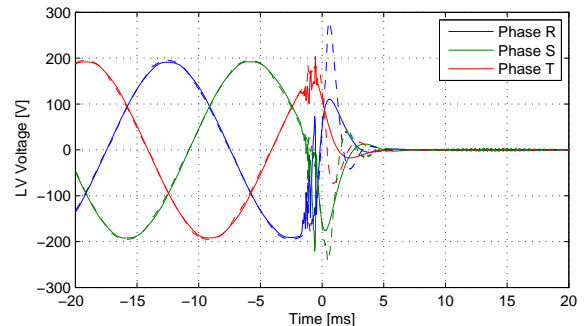
If an ideal breaker is used alone for the opening sequence, high overvoltages result from the simulation of the disconnection transient. Such high overvoltages are not in agreement with measurements. An accurate prediction of the disconnection transient and of the resulting overvoltages greatly affects the capability of the model to reach an accurate value of the residual fluxes.

The breaker model is highly empirical and is not based on any mathematical or physical consideration. More advanced breaker models where arcing, TRV and high frequency effects are more correctly modeled are reported in [17]–[19].

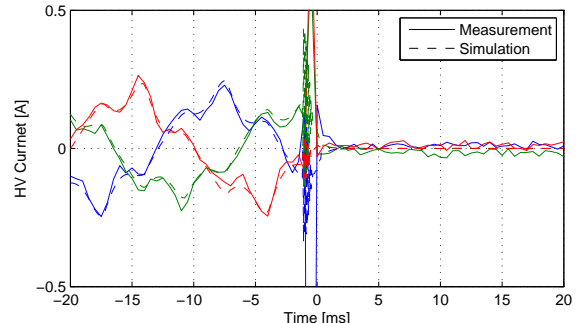
The dynamic of the circuit breaker is recorder by the measurement of the voltage on the transformer terminal. However, there is no benefit in representing the whole power system including the breaker model as a point by point voltage source: the transient during the ringdown is ruled by the exchange of energy between the reactive elements of the transformer itself that behave alternately as source and load, [14].

IV. RESULT COMPARISON

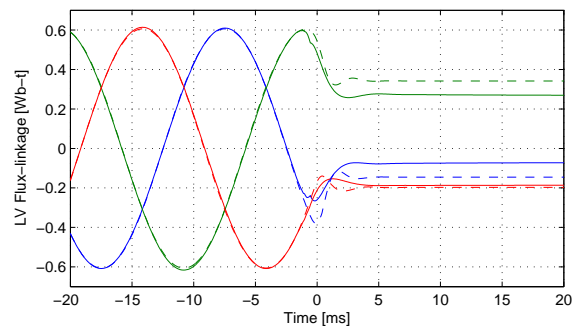
Measurements of de-energization and energization transients have been performed as detailed in II and reproduced with the model presented in III. The model parameters have not been adjusted to match the measured inrush peak, but derived as detailed in III and remain consistent through all the



(a) Phase voltage, low voltage side.



(b) Line current, high voltage side.



(c) Flux-linkage, low voltage side.

Fig. 7. Ringdown transient, waveforms.

simulations. While the breaker timing in the simulation can be exactly set, a stochastic difference between the desired and the real operation time of $\pm 1\text{ ms}$ is expected in the operation of the real breaker, as well a minimum unpredictable delay between the different phases. In the simulations, the breaker closing and opening time has been set to best match each measurement, still maintaining a simultaneous operation between the three poles of the breaker.

Ungrounded wye connection set severe constraints on the independent development of voltages and currents of the three phases as:

$$i_R(t) + i_S(t) + i_T(t) = 0 \quad (15)$$

$$\lambda_R(t) + \lambda_S(t) + \lambda_T(t) \approx 0 \quad (16)$$

with ≈ 0 reflecting the presence of a zero sequence flux flowing through a high impedance path. Such somehow opposing physical constraints stress even more the model as the three phases are not free to evolve independently but are highly

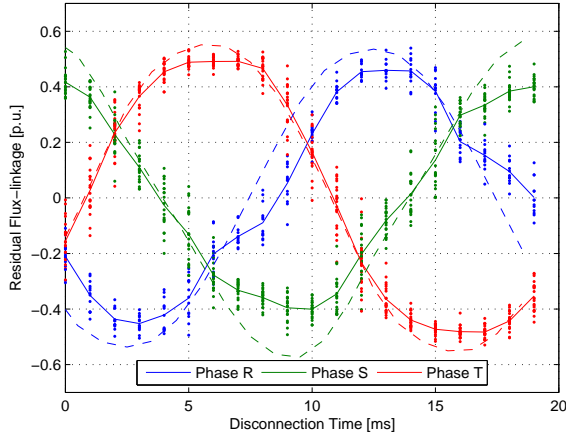


Fig. 8. Residual flux function of the disconnection time (dots: measurements, solid lines: average of measurements, dashed lines: simulation).

connected.

Flux-linkage is calculated here as integral of the voltage induced on the low voltage side. Such quantity is a direct indication of the flux in the core. The flux of each limb (legs and yokes) can be estimated from the model, but cannot be directly measured from the terminals.

The $time = 0$ in the next figures is synchronous to the triggering instant, that is the zero crossing of the voltage-to-ground of phase R on the high voltage side.

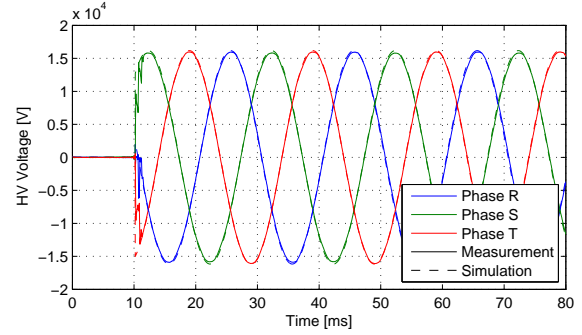
A. Ringdown Transient

Fig. 7 compares one case of measured and simulated disconnection transient. The steady state no-load condition are shown in the $20ms$ before the initiation of the transient. Steady state no-load current and flux-linkage are correctly predicted by the model. The disconnection transient is a high frequency transient due to the arcing in the breaker. The simple breaker model used fails to correctly predict all the details of the transient, however the main goal to reach a fairly accurate value of residual flux is achieved.

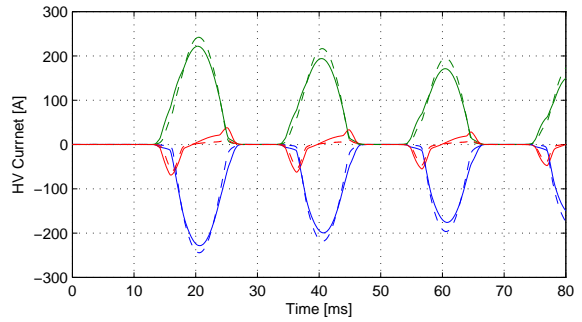
Fig. 8 gives an overview of the residual flux function of the disconnection time. A resolution of $1ms$ has been used to scan through one period ($0 - 19ms$). Such measurement has been repeated 20 times and the average of 20 points has been used. The agreement with simulation is reasonable considering the stochastic behavior of the breakers operation. The maximum residual flux is c.a. 50% the rated flux and is correctly predicted by the model. Such low value is in contradiction with normally assumed residual flux (75–90%) but is in agreement with previous findings, [14].

B. Inrush Transient

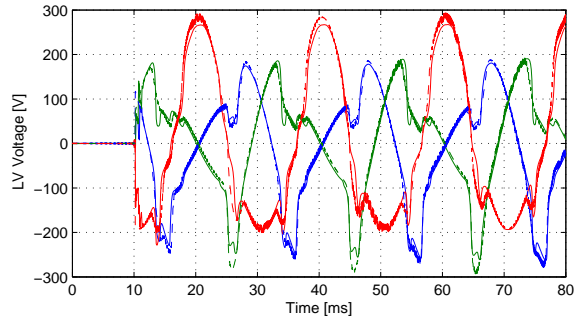
Fig. 9 shows the detailed comparison between measurements and simulation of the first three periods of an inrush transient. This case is one of the most severe case recorded on the ungrounded wye connected $300kVA$ transformer. The accuracy is very good, and the model is able to predict the amplitude of the first current peak and represent most of the



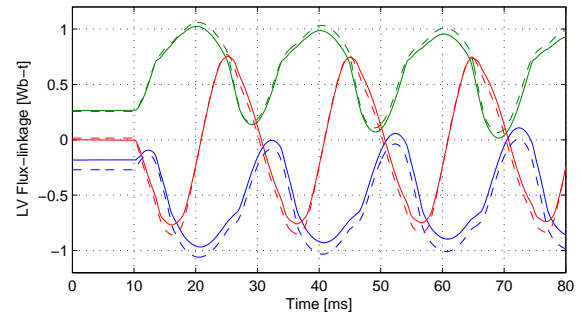
(a) Line voltage, high voltage side.



(b) Line current, high voltage side.

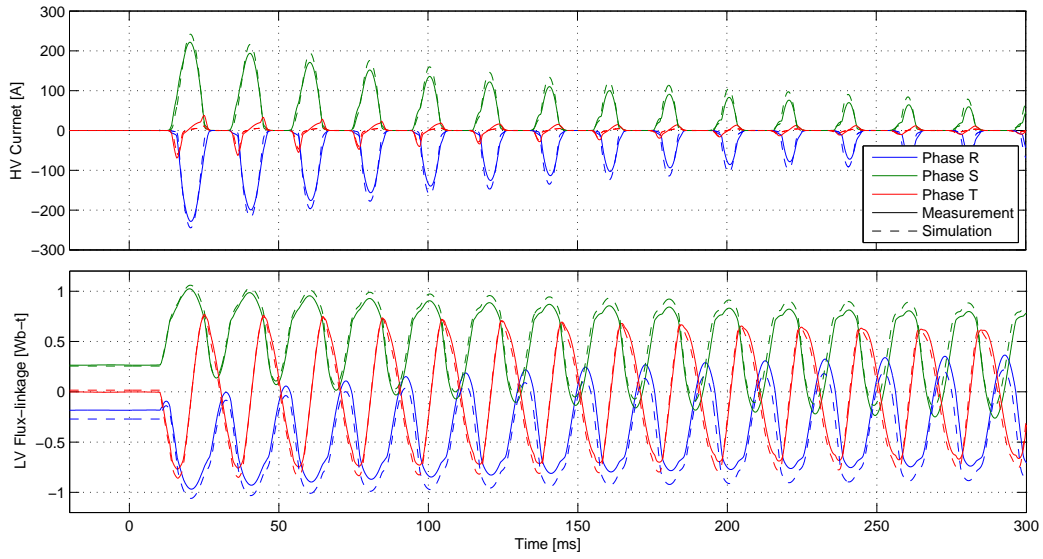


(c) Phase voltage, low voltage side.

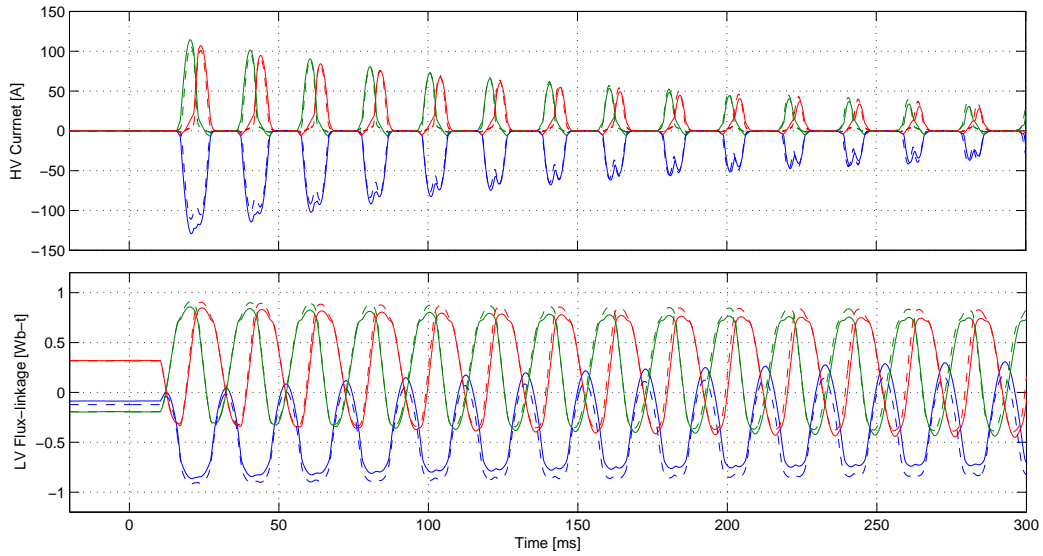


(d) Flux-linkage, low voltage side.

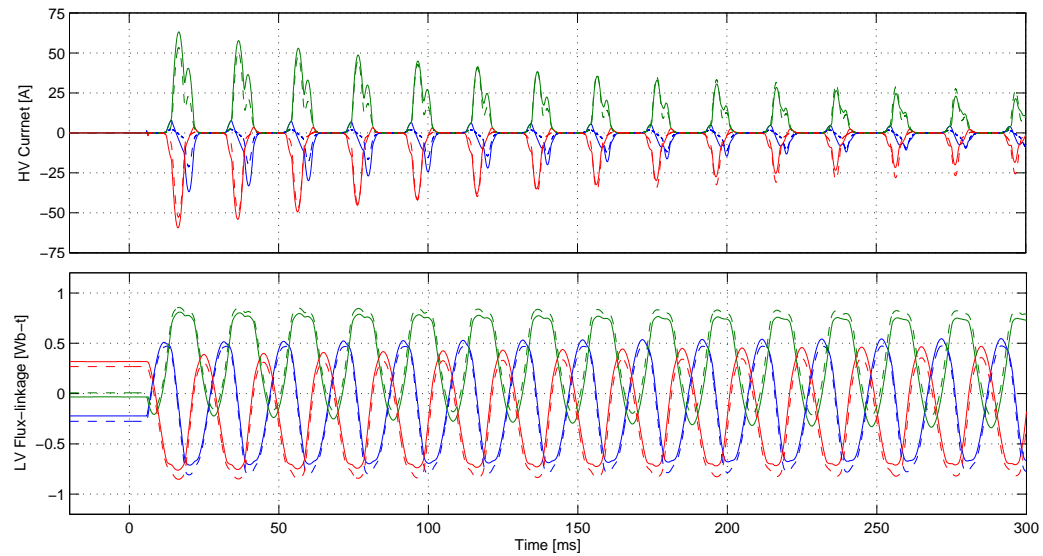
Fig. 9. Inrush transient, waveforms.



(a) $T_{OUT} = 1ms$, $T_{IN} = 10ms$.



(b) $T_{OUT} = 7ms$, $T_{IN} = 10ms$.



(c) $T_{OUT} = 4ms$, $T_{IN} = 5ms$.

Fig. 10. Inrush current and flux-linkage decay, waveforms.

details of the current and the highly distorted induced voltage. Initialization flux at the first instants of Fig. 9(d) is obtained from previous de-energization transient and is not very accurate for phase R due to the reasons described in the previous section; This could explain some of the inaccuracy of the model in predicting inrush transients. Fig. 10 gives a better overview of the performance of the model for three different amplitudes of inrush current first peak. The first fifteen periods are shown to reveal the capability of the model to correctly estimate the inrush current attenuation.

V. CONCLUSION

A test method and a novel transformer model able to estimate residual flux and inrush current has been presented. The model is not specialized for inrush current, but can be used in any transient simulation where transformers have to be modeled and saturation is a concern.

The overall agreement between measurements and simulation is very satisfactory with the proposed model and parameters estimation procedure being able to accurately reach residual flux and inrush current first peak, as well as decay ratio. The main limitation here is believed not related to the transformer model itself, but to a fairly poor breaker model; the investigation of a more performing breaker model is however outside the scope of the current work.

The proposed model has been extensively verified for its capability to correctly predict both residual flux value and energization transients. It has been common to only verify a model against a single inrush current measurement, however this is quite limiting as several parameters interact differently to determine the inrush peak and attenuation. The verification against three measurements with substantially different current development strengthens the broadness of the model. Future work involves the testing of the model for different transformer size and construction, as well as coupling scheme. Parameter sensitivity will also be investigated in a future work.

REFERENCES

- [1] F. de Leon and A. Semlyen, "Complete transformer model for electromagnetic transients," *IEEE Trans. Power Del.*, vol. 9, no. 1, pp. 231–239, 1994.
- [2] J. A. Martinez and B. A. Mork, "Transformer modeling for simulation of low-frequency transients," *2003 IEEE Power Engineering Society General Meeting, Conference Proceedings*, vol. 2, pp. 1223–1225, 2003.
- [3] —, "Transformer modeling for low- and mid-frequency transients - a review," *IEEE Trans. Power Del.*, vol. 20, no. 2 II, pp. 1625–1632, 2005.
- [4] H. W. Dommel and et.al., *Electromagnetic Transients Program Reference Manual (EMTP Theory Book)*. Portland, OR: Prepared for BPA, Aug. 1986.
- [5] W. Enright, O. Nayak, G. Irwin, and J. Arrillaga, "An electromagnetic transients model of multi-limb transformers using normalized core concept," in *IPST'97 - International Conference on Power System Transients, Seattle, Washington, June 22-26, 1997*, pp. 93 – 98.

- [6] W. Enright, O. Nayak, and N. Watson, "Three-phase five-limb unified magnetic equivalent circuit transformer models for PSCAD V3," in *IPST'99 - International Conference on Power System Transients, Budapest, Hungary, July 20-24, 1999*, pp. 462 – 467.
- [7] Y. Zhang, T. Maguire, and P. Forsyth, "UMEC transformer model for the real time digital simulator," in *IPST'05 - International Conference on Power System Transients, Montreal, Canada, June 19-23*, no. IPST05-77, 2005.
- [8] B. Mork, F. Gonzalez, D. Ishchenko, D. Stuehm, and J. Mitra, "Hybrid transformer model for transient simulation: Part I: development and parameters," *IEEE Trans. Power Del.*, vol. 22, no. 1, pp. 248–255, Jan. 2007.
- [9] —, "Hybrid transformer model for transient simulation: Part II: laboratory measurements and benchmarking," *IEEE Trans. Power Del.*, vol. 22, no. 1, pp. 256–262, Jan. 2007.
- [10] B. A. Mork, D. Ishchenko, F. Gonzalez, and S. D. Cho, "Parameter estimation methods for five-limb magnetic core model," *IEEE Trans. Power Del.*, vol. 23, no. 4, pp. 2025–2032, Oct. 2008.
- [11] H. K. Høidalen, B. A. Mork, F. Gonzalez, D. Ishchenko, and N. Chiesa, "Implementation and verification of the hybrid transformer model in atpdraw," *Electr. Power Syst. Res.*, vol. 79, no. 3, pp. 454 – 459, Mar. 2009, special Issue: Papers from the 7th International Conference on Power Systems Transients (IPST), 7th International Conference on Power Systems Transients.
- [12] E. Bjerkan, "High frequency modeling of power transformers," Ph.D. dissertation, NTNU, 2005.
- [13] S. V. Kulkarni and S. A. Khaparde, *Transformer engineering: design and practice*, ser. Power engineering. New York, N.Y.: Marcel Dekker, Inc., 2004, vol. 25.
- [14] N. Chiesa, A. Avendaño, H. K. Høidalen, B. A. Mork, D. Ishchenko, and A. P. Kunze, "On the ringdown transient of transformers," in *IPST'07 - International Conference on Power System Transients, Lion, France, June 4-7*, no. IPST-229, 2007.
- [15] N. Chiesa and H. K. Høidalen, "Modeling of nonlinear and hysteretic iron-core inductors in ATP," in *EEUG Meeting 2007, European EMTP-ATP Conference*, Leon, Spain, Sep. 2007.
- [16] —, "Hysteretic iron-core inductor for transformer inrush current modeling in EMTP," in *PSCC 2008, 16th Power Systems Computation Conference*, Glasgow, Scotland, Jul. 2008.
- [17] J. Kosmac and P. Zunco, "A statistical vacuum circuit breaker model for simulation of transient overvoltages," *IEEE Trans. Power Del.*, vol. 10, no. 1, pp. 294–300, Jan. 1995.
- [18] J. Helmer and M. Lindmayer, "Mathematical modeling of the high frequency behavior of vacuum interrupters and comparison with measured transients in power systems," in *Proc. ISDEIV. XVIIth International Symposium on Discharges and Electrical Insulation in Vacuum*, vol. 1, 21–26 July 1996, pp. 323–331.
- [19] M. Popov and E. Acha, "Overvoltages due to switching off an unloaded transformer with a vacuum circuit breaker," *IEEE Trans. Power Del.*, vol. 14, no. 4, pp. 1317–1326, Oct. 1999.

Nicola Chiesa was born in Italy in 1980. He received the M.S. degree in Electrical Engineering from Politecnico di Milano in 2005. In September 2005 he joined the Department of Electric Power Engineering at the Norwegian University of Science and Technology as a Ph.D. candidate.

Hans K. Høidalen was born in Norway in 1967. He received his MSc and PhD from the Norwegian University of Science and Technology in 1990 and 1998 respectively. He is now a professor at the same institution with a special interest on electrical stress calculations and modeling.